

Characteristics of zinc electrodeposits from acetate solutions

R. SEKAR* and SOBHA JAYAKRISHNAN

Central Electrochemical Research Institute, Karaikudi, 630 006 Tamilnadu, India

(*author for correspondence, e-mail: grsek2004@yahoo.com)

Received 18 April 2005; accepted in revised form 14 December 2005

Key words: acetate, electrodeposition, galvanostatic, non-cyanide, potentiodynamic polarization, zinc

Abstract

This paper deals with zinc plating from an acetate electrolyte and the resultant deposit properties. The addition of thiamine hydrochloride and gelatin to the plating bath improves the corrosion resistance and surface morphology of the zinc deposits. The XRD pattern obtained for electrodeposited zinc show a polycrystalline nature with a hexagonal structure. A uniform and pore free surface was observed under SEM analysis.

1. Introduction

Zinc is extensively used as a coating for iron and ferrous metal parts because zinc being anodic to iron and steel sacrificially protects the base metal at low cost [1]. Chromate conversion coatings further improve the protection, by enhancing the corrosion resistance, particularly by minimizing the formation of white corrosion products as well as providing a colour finish [2]. Deposition of zinc has been widely investigated using various approaches, which effectively lead to the preparation of coatings that differ in their macro and microstructure, texture, density, uniformity and corrosion resistance [3–6].

Presently zinc is electrodeposited from acid electrolytes [7–11] and non-cyanide alkaline electrolytes [12–15] as alternatives to those based on highly toxic cyanide. Various attempts have been made by different workers to study the different types of acid electrolytes. Weak acidic baths [16–17] are often used for bright zinc plating and are capable of producing decorative and functional deposits in rack and barrel applications. Electrodeposition of zinc from acetate electrolyte has not been reported, but acetate is used as a minor ingredient in some zinc plating electrolytes [18–20].

The authors have earlier reported data on the electrodeposition parameters of zinc from acetate based electrolytes [21–22]. In this paper results on bath characteristics, namely conductivity, throwing power, cathodic polarization and self-corrosion of zinc anodes and deposit characteristics such as adhesion, porosity, reflectivity, corrosion resistance crystal structure and surface morphology are reported.

2. Experimental details

The conductivity of the different solutions was determined by means of a digital conductivity meter (Model-TESTRONIX-15, India). Pretreated cold rolled steel specimens (6.25 cm^2) were subjected to cathodic polarization (galvanostatic method) studies in zinc plating baths A, B and C (Table 1) using a three electrode cell arrangement. The potential of the steel cathode at different current densities during zinc deposition were measured vs. SCE and E-I curves plotted. Throwing power was measured using a Haring and Blum cell [23–25]. This is a rectangular cell consisting of two sheet metal cathodes of $7.5 \times 5 \times 0.1 \text{ cm}$ size filling the entire cross section at both ends, and one perforated anode of the same size. The latter was placed between the cathodes so that its distance from one of the cathode was one fifth of its distance from the other. Values of throwing power for different solutions used were calculated using Field's formula.

$$\text{Throwing power}(\%) = \frac{K - C}{K + C - 2} \times 100$$

where C is the metal distribution ratio between the near and far cathode and K is the ratio of the respective distances of the far and near cathode from the anode.

Weighed zinc anodes (1 cm^2) were immersed in various baths and after specific periods, weight losses were determined by weighing after cleaning and drying the specimens [26].

The Bend test [27] was followed to evaluate the adhesion of the zinc coatings on steel. For determining the porosity of coatings of zinc on steel substrates

Table 1. Conductivity of various zinc plating baths

Bath	Composition/g l ⁻¹	Conductivity/ Ohm cm ⁻²
A	Zinc acetate	200
	Potassium acetate	60
	Aluminium sulphate	60
	Boric acid	40
B	Zinc acetate	200
	Potassium acetate	60
	Aluminium sulphate	60
	Boric acid: 40	40
C	Thiamine hydrochloride	3
	Zinc acetate	200
	Potassium acetate	60
	Aluminum sulphate	60
	Boric acid	40
D	Gelatin	3
	Zinc sulphate: 240	240
	Sodium acetate	30
E	Aluminium sulphate	30
	Zinc cyanide	60
	Sodium cyanide	23
	Sodium hydroxide	53

the Ferroxyl test was used [28]. The Ferroxyl solution was one of sodium chloride (50 g l⁻¹) and white gelatin (50 g l⁻¹), dissolved in distilled water at 45 °C. Filter paper strips of 25×25 mm area each were impregnated with the above solution and dried. Before testing the deposit porosity, the filter paper piece was dipped in the above solution and placed at different locations on the plated surface. After 10 min the papers were removed and placed in 10 g l⁻¹ solution of potassium ferricyanide. The porosity of each deposit was evaluated on the basis of the number of blue spots formed.

The zinc deposits of 10 µm thickness obtained from various baths were subjected to reflectivity measurement using a gloss meter referenced against a vacuum coated silver mirror, the reflectivity for which was set at 100% at an angle of 85°. The measurements were carried out at different points of the coating surface [29].

The electrodeposited specimens were masked to expose 1 cm² area on one side. A platinum foil (2.5×2.5 cm²) and saturated calomel electrode were employed as auxillary and reference electrode, respectively; 5% sodium chloride was used as test solution. The polarization behaviour was studied in the test electrolyte for zinc deposits of different thicknesses (3, 6, 12 and 18 µm). The working electrode was introduced into the test solution and it was allowed to attain a steady potential value. Anodic and cathodic polarization was carried out upto ±200 mV away from the OCP at a scan rate of 1 mV/s. E_{corr} and i_{corr} values were obtained from the plot of E vs. $\log i$ curves by Tafel extrapolation method.

X-ray diffraction patterns were obtained for zinc deposits obtained from various zinc plating baths at 30 and 40 °C. The deposits produced in the presence of additives and without additives were studied. The

samples were scanned at 30°–80° (2θ) at a scan rate of 1 degree per minute using CuK α ($\lambda = 1.5405 \text{ \AA}$) radiation. The peaks due to the different phases were identified and the corresponding lattice parameters calculated. In order to understand the nature of the deposits obtained, the deposits obtained from different electrolytes were studied visually and by using a Scanning Electron Microscope. SEM photographs were taken by using the Model JEOL-JSM-35 LF at 25 kV.

3. Results and discussion

3.1. Bath conductivity, cathodic polarization and throwing power

The composition of the various zinc plating baths investigated and their conductivity are given in Table 1. The conductivity values of acetate baths (Bath A, B, C) are much higher than those of sulphate baths and higher than that reported [30] for a cyanide bath. Generally, a plating bath having high conductivity is associated with low energy consumption and greater throwing power.

The potential of the steel cathode at different current densities during zinc deposition from different baths was measured vs. SCE (Figure 1). The potential in bath C exhibited more negative values at all current densities as compared to that in bath B and bath A. It can be seen

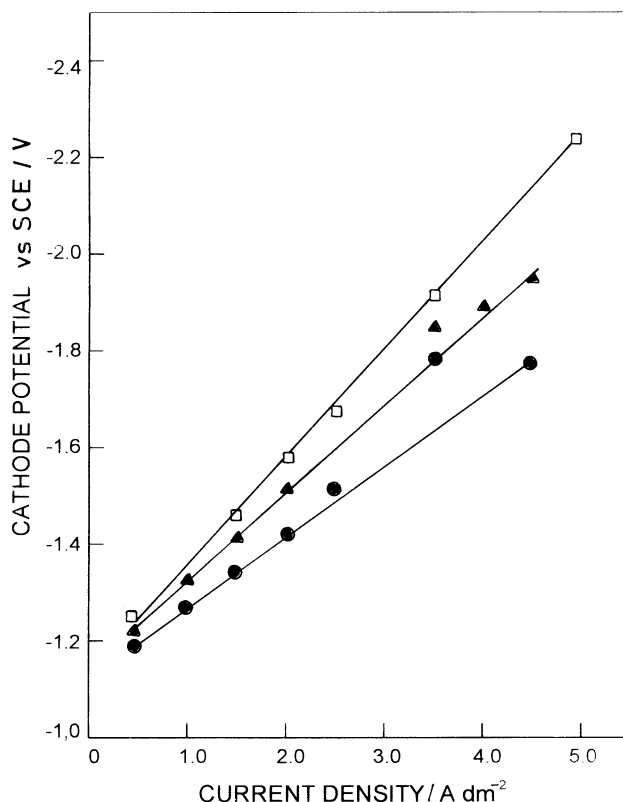


Fig. 1. Cathodic polarization curves during zinc deposition in Baths A, B, C at different current densities at 30 °C, pH 5. Bath A (●); Bath B (▲); Bath C (□).

that the electrolyte with gelatin polarizes the cathode surface to a greater extent [31]. The higher the polarization, the stronger is the adsorption on the active sites of the cathode surface.

Table 2 presents the variation of throwing power of bath A with current density and temperature. When temperature and current density increased, the throwing power of the bath clearly increased. This could be attributed to increase in cathodic polarization with increasing temperature and current density.

With the addition of thiamine hydrochloride 3 g l^{-1} as additive in Bath B it can be seen that high throwing power values are obtained at 30°C and at low current density, the throwing power decreases with increase in current density especially at high temperatures. This may be attributed to hydrogen evolution at high temperature and at high current densities. The decrease in throwing power could be attributed to the decrease in polarization, even though increase in temperature enhances the conductivity of the solution.

The variation of throwing power in bath C, which contains 3 g l^{-1} gelatin as additive, shows that throwing power initially increases at all current densities with temperature from 30 to 40°C but decreases at 50°C . This may be due to the additive decomposition at high temperatures.

3.2. Self-corrosion of zinc anodes

Figure 2 represents the variation of weight loss of zinc with time in different plating baths at pH 5 and 30°C when kept immersed. There was a uniform increase in weight loss with time in bath A. The weight loss was found to be less in the presence of thiamine hydrochloride (bath B). Bath C exhibited minimum amount of weight loss as compared to the baths A and B. Therefore we may conclude that both thiamine hydrochloride and gelatin act as inhibitors.

3.3. Adhesion, porosity and reflectivity

The deposits from all the three baths were found to withstand the bend test showing that the keying of the deposit to the base metal was very good in all cases.

Table 2. The percentage throwing power for electrodeposition of zinc from various acetate baths and pH 5

Bath	Temperature/ $^\circ\text{C}$	Current densities/ A dm^{-2}			
		1.0	2.0	3.0	4.0
A	30	0.5	1.2	2.2	5.2
	40	0.7	1.8	5.0	6.1
	50	1.0	2.3	7.1	9.6
B	30	22.1	15.6	8.3	7.0
	40	15.6	12.0	5.5	5.1
	50	5.4	5.9	2.6	2.1
C	30	9.0	7.0	3.7	3.0
	40	9.7	8.4	7.0	3.8
	50	4.3	2.9	1.8	1.2

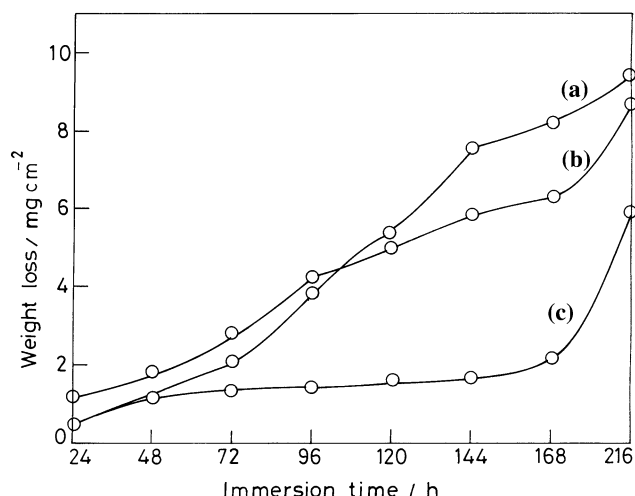


Fig. 2. Self-corrosion of zinc anodes in zinc plating baths with and without additives (a) Bath A; (b) Bath B; (c) Bath C.

Ferroxyl test results revealed that zinc electrodeposits from all the three baths were non-porous at $6\text{ }\mu\text{m}$ thickness level showing that the deposits are compact and fine grained in nature.

The percentage reflectivity for the zinc deposits produced under various conditions showed that the additive free bath (bath A) shows the lowest value of reflectivity (16.8%) as compared to 85% reflectivity for the deposit from thiamine hydrochloride containing bath (bath B) followed by 76% reflectivity for the deposit from gelatin containing electrolyte (bath C).

3.4. Potentiodynamic polarization method

On a zinc electrodeposit anodic and cathodic polarization experiments were carried out upto $\pm 200\text{ mV}$ away from open circuit potential at 1 mV s^{-1} . From the electrochemical theory of corrosion, corrosion current densities can be obtained by extrapolating the linear segments of cathodic and anodic Tafel plots.

Figure 3 presents the typical potentiodynamic polarization curves for deposits obtained from bath A, B and C of $12\text{ }\mu\text{m}$ thickness. There is no significant change in corrosion potential for the deposits obtained from the three baths (A, B and C) (Table 3). But the corrosion current was lower for the deposits produced from the baths containing thiamine hydrochloride followed by gelatin whereas the corrosion current is high for the deposit produced from the bath without additive.

3.5. X-ray diffraction and scanning electron microscopy

Figure 4(a)–(c) shows X-ray diffraction patterns of the zinc electrodeposits obtained from the three baths at 30°C . All the deposits are crystalline in nature and have hexagonal structure. The observed ' d ' value (Tables 4 and 5) is in good agreement with the standard values for zinc deposition (Joint Committee on Powder Diffraction System/ASTM File No.1-*40831Zn). Figure 4(a)

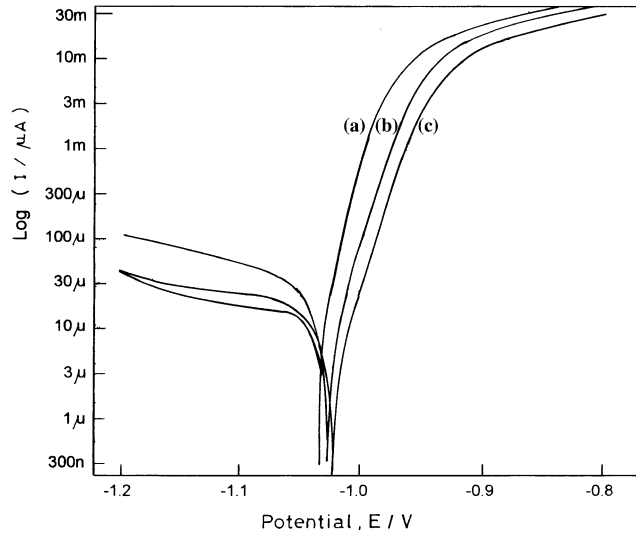


Fig. 3. Typical potentiodynamic polarization curves for (12 μm) zinc deposits in 5% NaCl solution (a) Bath A; (b) Bath B; (c) Bath C.

exhibited that the reflection from (103) plane was more predominant compared to other peaks. Reflection from the (100) plane was predominant for the deposit obtained from the thiamine hydrochloride bath (Figure 4(b)). The reflection from the (100) plane was predominant for the deposit obtained from the bath containing gelatin as additive (Figure 4(c)).

When the bath temperature is raised to 40 $^{\circ}\text{C}$, in all the three baths, the reflections from (101) plane was predominant as shown in Figure 5(a)–(c). The peak intensity of (101) plane increases when additives such as thiamine hydrochloride and gelatin are added to the initial bath A. The gelatin layer may decrease the hydrogen adsorption on the active zinc sites and increase the current efficiency. The high current efficiency may be related to the preferred texture (101) for the deposits having relatively fewer imperfections in crystal structure [32].

Figure 6(a) shows the typical surface morphology of a zinc deposit obtained from bath A at 30 $^{\circ}\text{C}$. The main

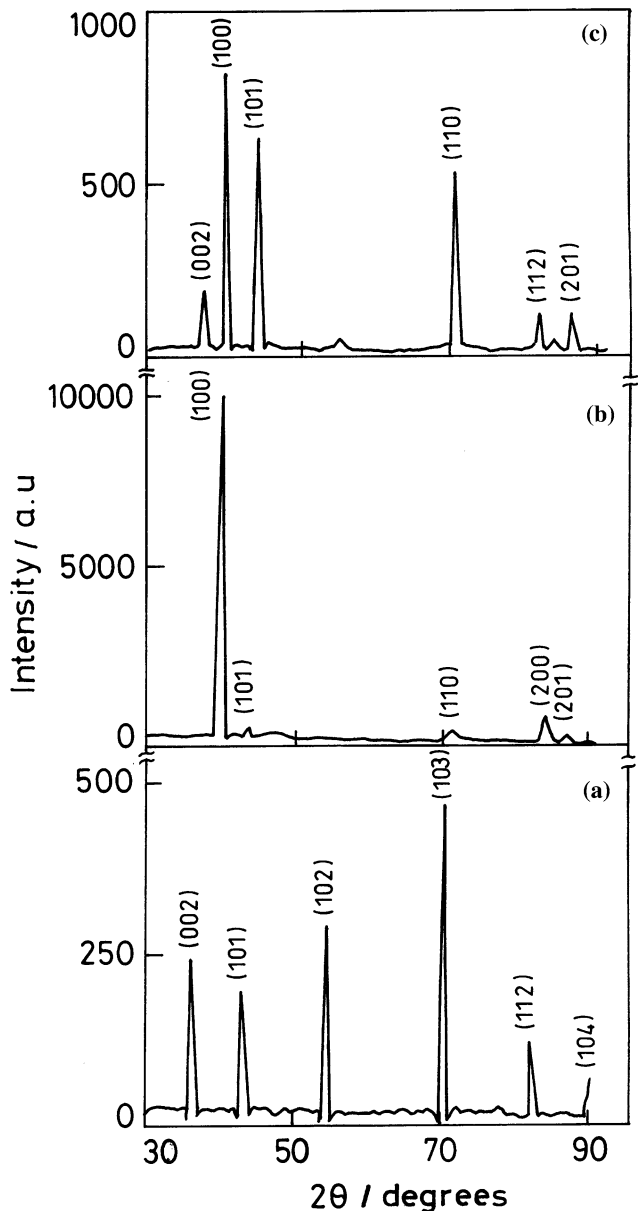


Fig. 4. XRD pattern for zinc deposits obtained at 30 $^{\circ}\text{C}$ from (a) Bath A; (b) Bath B; (c) Bath C.

Table 3. Parameters derived from E -log i curves for different zinc deposits obtained from different thicknesses in 5% NaCl solutions at 1 mV s^{-1} at 30 $^{\circ}\text{C}$

Deposit from bath	Thickness/ μm	vs. SCE E_{corr} /mV	E/mV	Corrosion current density/ $\mu\text{A cm}^{-2}$	Tafel slopes	
					Anodic/mV decade $^{-1}$	Cathodic/mV decade $^{-1}$
A	3		-1005	8.25	13	47
B			-1108	7.00	29	32
C			-1035	7.50	39	58
A	6		-1015	7.2	19	87
B			-1029	6.2	32	32
C			-1009	6.6	19	45
A	12		-1034	6.1	19	65
B			-1020	5.3	23	58
C			-1031	5.8	29	39
A	18		-1038	5.6	32	58
B			-1040	4.9	32	64
C			-1022	5.3	23	55

Table 4. X-ray diffraction data for electrodeposited zinc obtained at 30 °C

Bath	'd' observed	'd' standard	hkl	Lattice parameters/ nm	<i>c/a</i> ratio	Structure		
							a	c
A	2.466	2.473	002	2.6698	4.9326	1.8475	Hexagonal	
	2.088	2.091	101					
	1.682	1.687	102					
	1.340	1.342	103					
	1.171	1.172	112					
	1.089	1.090	104					
B	2.302	2.308	100	2.6578	4.9326	1.8558	Hexagonal	
	1.152	1.153	200					
	2.083	2.091	101					
C	2.466	2.473	002	2.6501	4.8911	1.8400	Hexagonal	
	2.302	2.308	100					
	2.083	2.091	101					
	1.330	1.332	110					
	1.169	1.172	112					
	1.122	1.123	201					

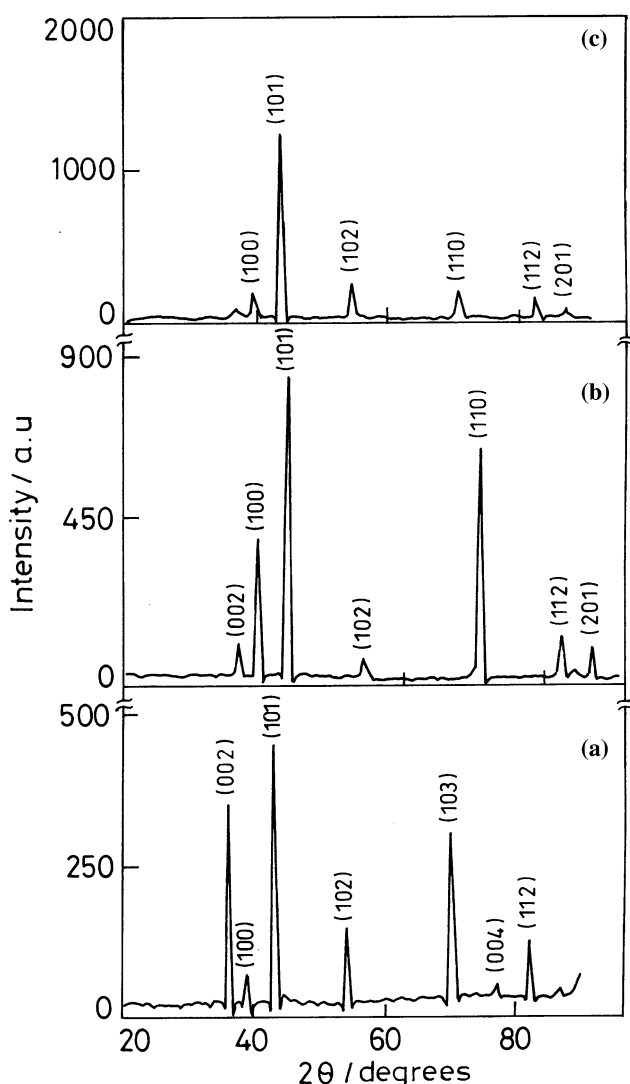


Fig. 5. XRD pattern for zinc deposits obtained at 40 °C from (a) Bath A; (b) Bath B; (c) Bath C.

Table 5. X-ray diffraction data for electrodeposited zinc obtained at 40 °C

Bath	'd' observed	'd' standard	hkl	Lattice parameters/ nm	<i>c/a</i> ratio	Structure		
							a	c
A	2.479	2.473	002	2.6642	4.9583	1.8610	Hexagonal	
	2.092	2.091	101					
	1.688	1.687	102					
	1.341	1.342	103					
	1.172	1.172	112					
B	2.308	2.308	100	2.6649	4.9568	1.8600	Hexagonal	
	2.092	2.091	101					
	1.333	1.332	110					
	1.172	1.172	112					
C	2.296	2.308	100	2.6515	4.9507	1.8671	Hexagonal	
	2.083	2.091	101					
	1.679	1.687	102					
	1.335	1.332	110					

feature is a predominance of hexagonal platelets of 10–20 µm in size [33, 34]. Figure 6(b) shows at 40 °C a slight increase in grain size.

Figure 6(c) shows that addition of thiamine hydrochloride 3 g l⁻¹ (bath B) at 30 °C produced a different surface morphology. The platelet size was reduced to produce a different morphology and fine grain size. It was characterized by clusters of non-uniform large nodules growing on the surface. Figure 6(d) shows that 40 °C the grain size becomes larger. In general, a dense compact and fine grained structure improves corrosion resistance.

Figure 6(e) shows that the addition of 3 g l⁻¹ gelatin at 30 °C produced a fine grained structure which extended throughout the surface. The deposits obtained from gelatin containing baths are fine and of a dense surface morphology. The coating was equiaxed but was found to be slightly oriented towards the (101) plane by XRD analysis. It is also possible that gelatin may coat some zinc planes and prevent further growth. Figure 6(f) shows a fine fibre like structure, obtained at 40 °C.

4. Conclusion

It may be concluded that smooth uniform dense white and highly adherent deposits of zinc be electroplated from an acetate bath. Bright deposits with good throwing power, high cathodic polarization, high electrolyte conductivity and minimum amount of zinc self-corrosion can be obtained from this electrolyte with the addition of thiamine hydrochloride and gelatin as bath additives.

The corrosion characteristics of zinc deposits analysed by potentiodynamic polarization measurements shows that the deposits obtained from both thiamine hydrochloride and gelatin containing baths exhibited low corrosion current. This may be related to the pore free,

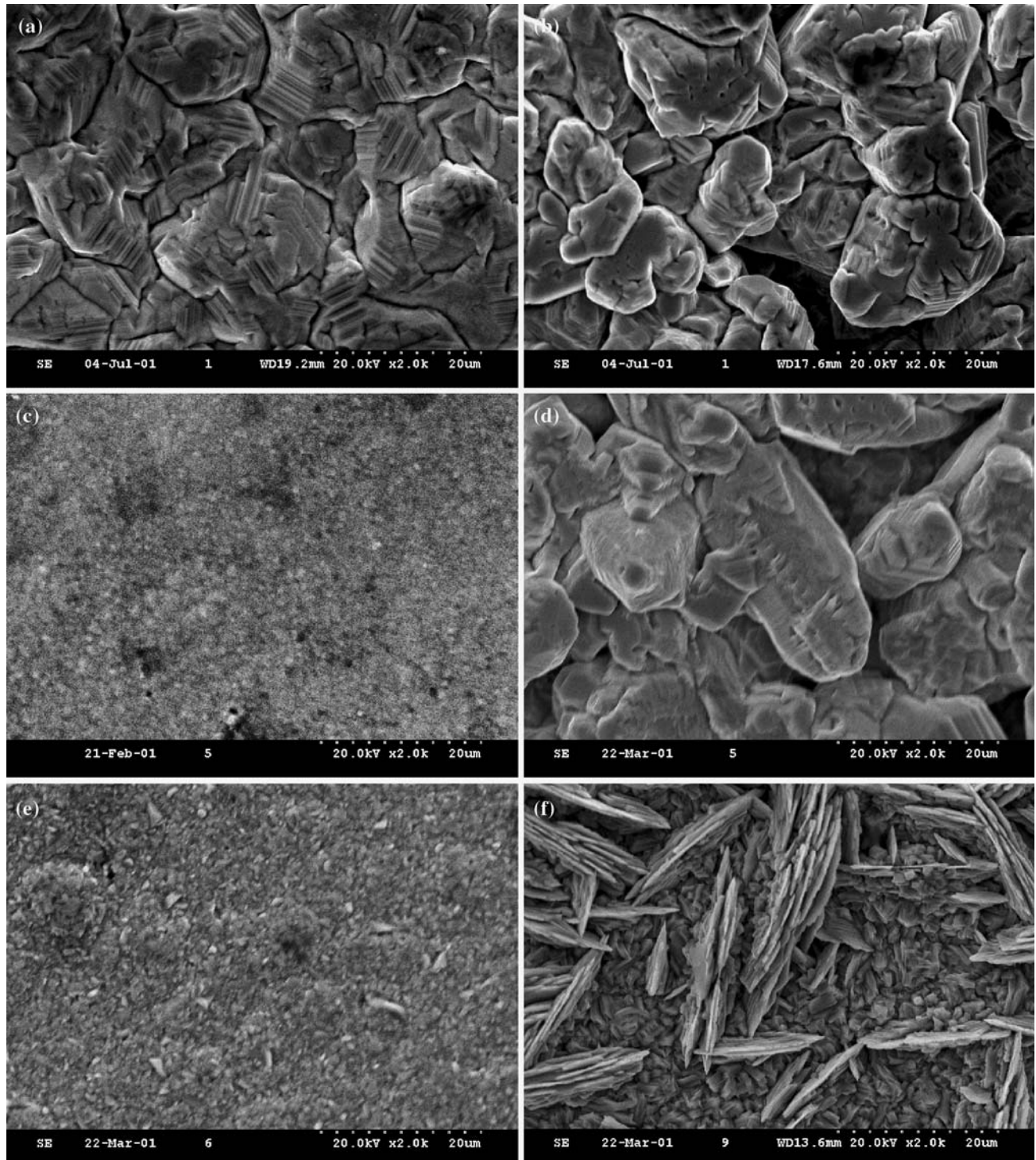


Fig. 6. SEM photograph of zinc deposit obtained at: (a) 30 °C from "Bath A" at 2 A dm^{-2} ; (b) 40 °C from "Bath A" at 2 A dm^{-2} ; (c) 30 °C from "Bath B" containing 3 g l^{-1} THC at 3 A dm^{-2} ; (d) 40 °C from "Bath B" containing 3 g l^{-1} THC at 3 A dm^{-2} ; (e) 30 °C from "Bath C" containing 3 g l^{-1} gelatin at 3 A dm^{-2} ; (f) 40 °C from "Bath C" containing 3 g l^{-1} gelatin at 3 A dm^{-2} .

compact and fine grained structure and high reflective index values of the deposits.

X-ray diffraction analysis reveals that the additive free deposits exhibited predominance of the (103) plane at 30 °C, whereas with introduction of thiamine hydrochloride and gelatin as additives the (100) plane was

predominant. But the deposits obtained from all baths at 40 °C exhibited a predominance of the (101) plane. SEM studies show that fine grained deposits are obtained from baths containing thiamine hydrochloride or gelatin (3.0 g l^{-1}) at 30 °C, thereby showing that these compounds act as grain refiners.

References

1. H. Geduld, *Zinc Plating* (Finishing Publications Ltd., England, 1998).
2. N.M. Martyak, J.E. Mccaskie and L. Harrison, *Met. Finish.* **94** (1996) 65.
3. Yu.S. Gerasimenko, M.V. Nechai and N.A. Belousova, *Mater. Sci.* **35** (1999) 273.
4. K. Raeissi, M.A. Golozar, A. Saatchi and J.A.SZ Punar, *Trans. Inst. Met. Fin.* **83** (2005) 119.
5. Y.B. Yim, W.S. Hwang and S.K. Hwang, *J. Electrochem. Soc.* **142** (1995) 2604.
6. Xingpu Ye, J.P. Celis, M. De Bonte and J. Roos, *J. Electrochem. Soc.* **141** (1994) 2698.
7. F. Hanna and H. Noguchi, *Met. Finish.* **86** (1998) 33.
8. E. Gomez, C. Muller, M. Sarret, E. Valles and J. Pregonas, *Met. Finish.* **90** (1992) 87.
9. T.V. Venkatesha, J. Balachandra, S.M. Mayanna and R.P. Dambal, *Plat. Surf. Fin.* **74** (1987) 77.
10. M. Pushpavanam and B.A. Shenoi, *Met. Finish.* **75** (1997) 29.
11. H.H. Geduld and R.O Hull, *Met. Finish.* **72** (1974) 35.
12. A. Ramachandran and S.M. Mayanna, *Met. Finish.* **90** (1992) 61.
13. V. Ravindran and V.S. Muralidharan, *Bull. Electrochem.* **16** (2000) 60.
14. S.V. Kulkarni, *Trans. Met. Finish. Assoc. India* **8** (1999) 205.
15. R.M. Krishnan, S.R. Natarajan, V.S. Muralidharan and G. Singh, *Met. Finish.* **80** (1991) 15.
16. K.P. Bellinger, *Plating* **56** (1969) 1135.
17. E.A. Blount, *Electroplat. Met. Finish.* **83** (1985) 33.
18. E.J.Smith, in F.A. Lowenheim (Ed.), 'Modern Electroplating', (J.Wiley & Sons, N.Y., 1963), p. 396.
19. Kyowa Hokko koggo Co. Ltd., Japanese Pat 29946 (1969).
20. Jujisawa Pharmaceutical Co. Ltd., Japanese Pat 7122084 (1967).
21. R. Sekar, S. Sriveeraraghavan and R.M. Krishnan, *Bull. Electrochem.* **15** (1999) 219.
22. R. Sekar, C. Kala and R.M. Krishnan, *Trans. Inst. Met. Fin.* **80** (2002) 173.
23. B.E. Conway and J.O'M. Bockris, *Plating* **46** (1959) 371.
24. H. Silman, G. Isserlis and A.F. Averill, *Protective and Decorative Coatings for Metals* (Finishing Publications Ltd., Teddington, England, 1978), p. 6.
25. S. Shawki, F. Hanna and Z.A. Hamid, *Met. Finish.* **85** (1987) 59.
26. R.M. Krishnan 'Some aspects of the electrodeposition of zinc, copper and copper zinc alloys', Ph.D.Thesis (Indian School of Mines, Dhanbad, 1986).
27. ASTM Test Method B571-84, Adhesion of metallic coatings (1995).
28. ASTM Test Method B689-81, Electroplated Engineering, Nickel coatings (1985).
29. ASTM D523-89 (1999), Standard Test Method for Specular Gloss, 06.01 (2001) 35.
30. M. Chandran, R. Lekshmana sarma and R.M. Krishnan, *Trans. Inst. Met. Fin.* **81** (2003) 207.
31. P.A. Adcock, A. Quillinan, B. Clark, O.M.G. Newman and S.B. Adelolu, *J. Appl. Electrochem.* **34** (2004) 771.
32. D.S. Baik and D.J. Fray, *J. Appl. Electrochem.* **31** (2001) 1141.
33. D. Vasilakopoulos, M. Powonshian and N. Spyrellis, *Trans. Inst. Met. Fin.* **79** (2001) 107.
34. K. Raeissi, A. Saatchi and M.A. Golozar, *J. Appl. Electrochem.* **33** (2003) 635.